Composites Part B 91 (2016) 522–538

Contents lists available at ScienceDirect

Composites Part B

journal homepage: www.elsevier.com/locate/compositesb

Impact damage tolerance of thermoset composites reinforced with hybrid commingled yarns

Erdem Selver [a, b], Prasad Potluri [b, *], Paul Hogg [c], Costas Soutis [b]

[a] Department of Textile Engineering, Kahramanmaraş Sütçü İmam University, Kahramanmaraş 46100, Turkey
[b] Northwest Composites Centre, University of Manchester, Manchester M13 9PL, UK
[c] Royal Holloway, University of London, Egham, Surrey TW20 0EX, UK

ARTICLE INFO

Article history:
Received 8 October 2014
Received in revised form
13 December 2015
Accepted 23 December 2015
Available online 3 February 2016

Keywords:
A. Hybrid
A. Fabrics/textiles
B. Impact behaviour
B. Damage tolerance
A. Commingled yarn

ABSTRACT

This paper examines the potential of low-cost thermoplastic fibres in improving the impact damage resistance and damage tolerance of thermoset (glass-epoxy) composites. Polypropylene (PP) fibres, commodity fibres without any surface modifications, have been incorporated at tow-scale with the aid of air jet commingling process. Glass-PP hybrid yarns with varying proportion of PP fibres (0–35%) are converted into several non-crimp cross-ply laminates and a plain-woven laminate. Damage resistance in terms of damage area and depth are assessed for low energy (20–50 J) as well as high energy (500 J) drop-weight impacts; damage tolerance is assessed through Compression after Impact (CAI) tests. Overall density of the composite laminate has reduced by 16% due to the introduction of PP fibres; at the same time total absorbed energy has increased by 22% during a high velocity impact test due to a toughing mechanism by PP fibres. Non-crimp laminates absorbed more energy at low velocity impacts in comparison to woven laminates, possibly due to extensive tow-level delaminations. On the other hand, a much larger dent depth was observed in the woven laminate after low energy impact. Compression after Impact (CAI) tests indicated that woven laminates retained 83% of compressive strength while non-crimp laminates retained 50–60%, depending on proportion of thermoplastic fibres, and standard glass fibre laminates retain around 45%. Fibre damage has been significantly reduced during impact loading in case of hybrid laminates due to the cushioning effect offered by lower modulus PP fibres.

1. Background

Fibre reinforced composite materials have seen a rapid growth in the last two decades [1,2] in aerospace, automotive, wind energy, marine and civil engineering applications. However, their susceptibility to impact damage is still of main concern since the induced damage can significantly reduce compressive strength of the structure [3–6]. Low or high velocity impact damage can be introduced as a result of events such as dropping of tools during maintenance or due to impact of hailstones, runway debris, bird strike, etc. during service [7].

There is an increasing trend to use thermoplastic composites due to their higher damage tolerance [8]. Previous research showed that thermoplastic matrix composites (Carbon/PEEK or Glass/PEEK) exhibited higher compression and compression after impact (CAI) properties with higher strains to failure in comparison to thermoset composites [9,10]. One of the recent studies showed that carbon fabric laminates with different thermoplastic resins (PEEK and PPS) provided smaller delaminated areas than laminates with epoxy resin after low velocity impact tests; this result is due to tougher matrix system in thermoplastic composites [11]. However, high resin viscosity in thermoplastics is a problem to impregnate the reinforcement fibres in tightly woven or unidirectional composites [12–15]; thermoset composites provide easier processing due to lower resin viscosity and that leads to a lower void content. Both the material and tooling costs for processing thermoplastic composites are higher than for thermoset composites [16]. This research is aimed at combining the benefits of lower material and processing costs of thermosets with the toughness of thermoplastics. Through hybridisation of reinforcing fibres with low-cost commodity thermoplastic fibres, damage tolerant composites may be developed for applications where expensive prepreg toughening solutions are not justified. Hybridisation of reinforcing fibres with lower density fibres (for impact loading) is analogous to

* Corresponding author. Tel.: +44 161 306 4128.
E-mail address: Prasad.potluri@manchester.ac.uk (P. Potluri).

http://dx.doi.org/10.1016/j.compositesb.2015.12.035

Table 1
Yarn specifications.

	Polypropylene	E glass
Yarn Number (T)[a]	33.3 tex	600 tex
Average filament diameter (d)[b]	25.3 μm	12.5 μm
Number of filaments (n)[b]	72	1950
Yarn density (ρ)[a]	0.91 g/cc (910 kg/m^3)	2.59 g/cc (2590 kg/m^3)
Yarn cost per kg (Cm)[a]	1-2 £	1-2 £
Yarn cost per m^3 (Cv)[a]	910 £	2590 £

[a] From yarn suppliers [50,51].
[b] Measured using Zeiss Smart SEM software during taking yarn cross-section images with SEM.

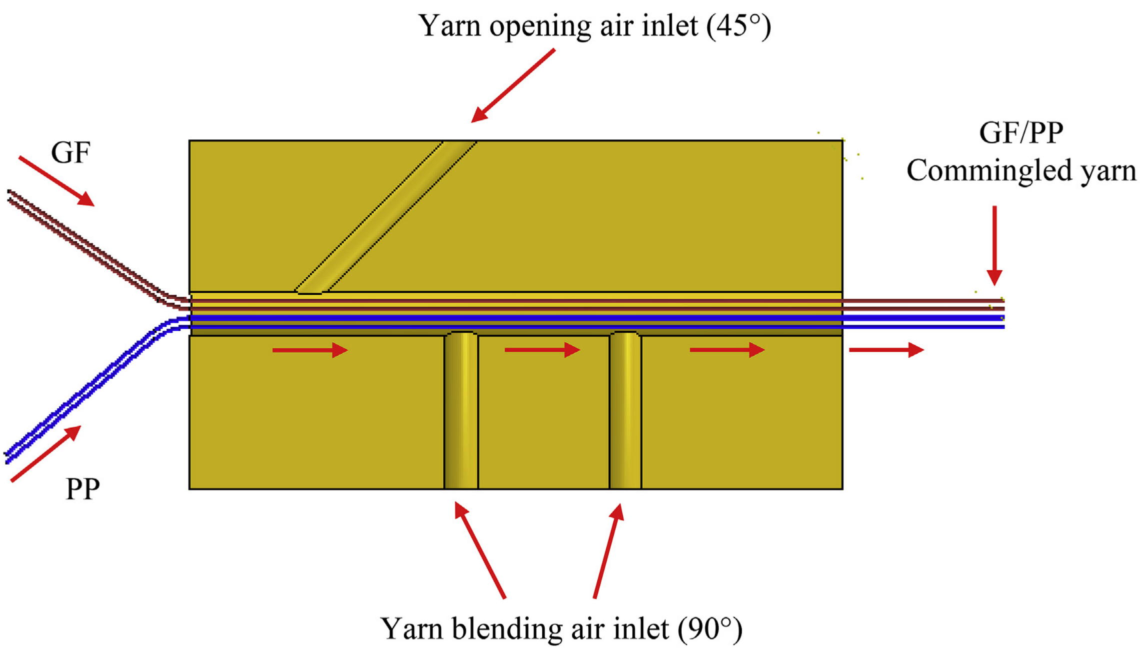

Fig. 1. Commingling nozzle cross-section.

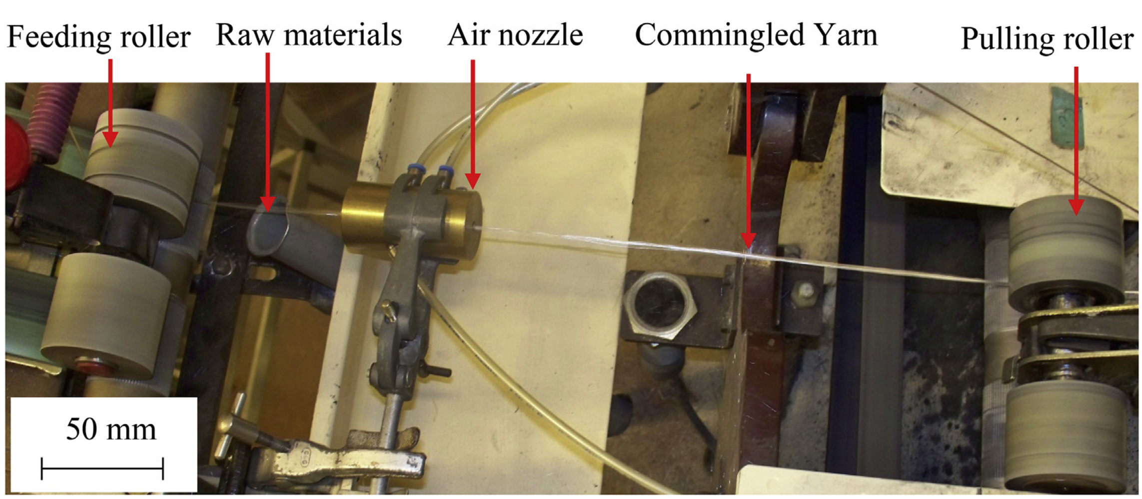

Fig. 2. Commingling yarn processing line at The University of Manchester.

combining reinforcing skins with lightweight foam in sandwich construction (for bending loads).

1.1. Hybrid yarns in composites

Impact energy absorption capacity of composite laminates may be increased by combining brittle (glass or carbon) fibres with higher strain-to-failure fibres such as aramid, high molecular weight polyethylene and conventional thermoplastic fibres [17–20]. Fibre hybridisation may be achieved by a commingling process in which high performance fibres and thermoplastic yarns are mixed with the influence of air flow through a suitably designed nozzle [21,22]. Almost any combination of glass (GF) or carbon fibres (CF) reinforcement and thermoplastic fibres can be mixed for

Table 2
Commingled yarn with different polypropylene ratios.

Sample code	PP fibre V_f(%)	PP fibre W_f(%)	Glass fibre V_f(%)	Glass fibre W_f(%)	Yarn linear density(tex)
GPP1	20	6	80	94	633
GPP2	28	12	72	88	666
GPP3	35	18	65	82	699

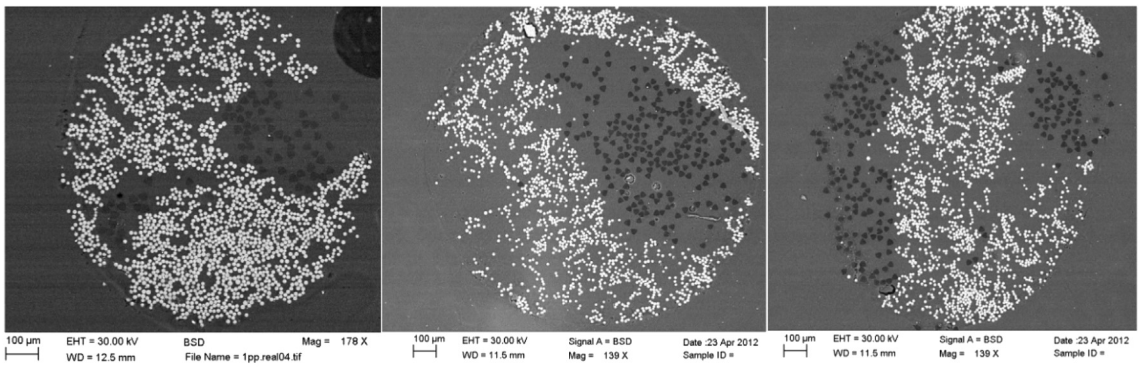

(a) (b) (c)

Fig. 3. Commingled yarn cross-sections E-glass fibres appear white: a) GPP1, b) GPP2, c) GPP3 sample.

structural applications using commingling method [23–27]. Commingled yarns are mainly used in thermoplastic composites in order to achieve optimum impregnation and consolidation quality due to their uniform mixture [28–30]. However, comingling yarns may also be used in conjunction with thermoset matrix in order to improve damage tolerance [31]. Addition of thermoplastic fibres helps in improving plastic deformation which can lead to an increase in the load sharing capacity of the structure [32–34].

1.2. Compression after impact strength

Low velocity drop-weight impact and compression-after-impact (CAI) tests are mainly used to evaluate damage resistance and tolerance of composite structures [35–37]. Atas and Sayman [38] observed that damage mechanism of laminates can be evaluated from energy profile diagram, images of impact-induced specimens and force-deflection curves. Mili and Necib [39] investigated impact response of non-crimp laminates made from different laminate sequences. They observed that stacking sequence did not affect the impact behaviour of laminates whilst changing the number of 0° plies influenced the central deflection of laminates during impact loading. Aktas et al. [40]analysed impact performance of laminates made from $[0/90/0/90]_s$ and $[0/90/+45/45]_s$ stacking sequences. Both systems absorbed similar amount of energies whilst penetration threshold for $[0/90/0/90]_s$ laminate was bigger than for $[0/90/+45/45]_s$ laminate. Lower energy levels caused delamination and matrix cracks while higher energy levels promoted fibre breakages for both sequences. Schrauwen and Peijs [41] compared impact performance of laminates made from brittle and ductile matrices with various fibre architecture; the authors observed that multi-axial laminates

Fig. 4. Glass fibre placement for a $[0, 90]_7$ configuration at the Manchester tow placement machine [50].

Table 3
Properties of the $[0/90]_7$ non-crimp and woven composite specimens.

Composite system code	Glass fibre V_f(%)	PP fibre V_f(%)[a]	Density (g/cm^3)	Thickness (mm)
GFC	59.5	–	2.033 (2.007)	4.62
12PPC	50.9	12.7	1.868 (1.851)	5.31
18PPC	46.9	18.2	1.790 (1.781)	5.86
22PPC	41.4	22.3	1.700 (1.692)	6.65
12PPW	44.8	11.2	1.770 (1.768)	5.51

( ) Rule of mixture prediction for density.
[a] The PP fibre volume fraction in the composite defines the composite codes.

Table 4
Tensile test results of E-glass-PP dry yarn.

Sample code	Glass fibre (V_f%)	Density (g/cm^3)	Modulus (GPa)	Tensile strength (MPa)	Strain at break (mm/mm)
PP	–	0.91	0.62 (±0.06)	199 (±5.0)	1.82
GF	100	2.59	48.7 (±1.45)	1026 (±54)	0.03
GPP1	80	2.26 (2.26)[a]	41.0 (±1.14)	785 (±10)	1.32
GPP2	72	2.10 (2.11)[a]	36.8 (±1.03)	690 (±41)	1.47
GPP3	65	1.97 (2.00)[a]	31.2 (±1.90)	615 (±52)	1.49

[a] Rule of mixture prediction for density. Density of yarns was calculated experimentally using ASTM D792 -08 standard using Mettler Toledo analytical balance [53].

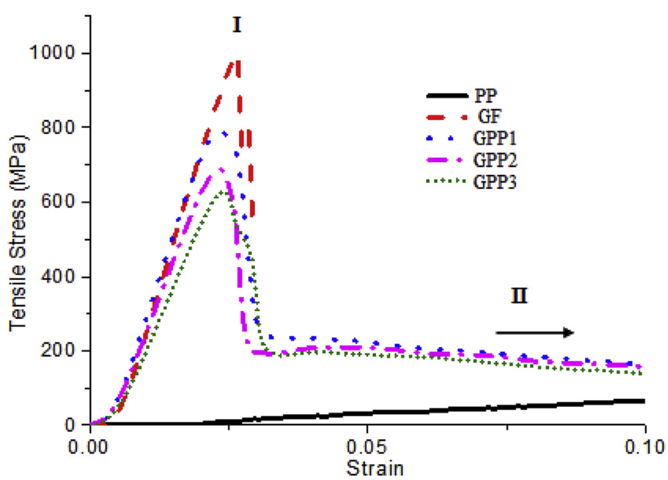

Fig. 5. Stress-strain curves of the different reinforcement yarns.

had higher penetration energies than woven laminates whilst matrix ductility did not make clear effect; fibre fracture rather than matrix failure has been found to be mainly responsible for absorbing the penetration energy. Woven laminates had smaller impact damage areas than multi-axial laminates due to delaying delamination, while ductile matrix laminates had smaller damage areas as brittle matrix laminates. Bibo and Hogg [42] claimed that fibre architecture controls the fracture mechanism of laminates since controlling the fracture mechanism helps to control the damage tolerance of composite laminates. Woven composite laminates have higher impact and damage tolerance than non-crimp laminates due to reduced impact damage which benefit from the yarn interlacement in woven laminates. However, their poor in-plane shear and low tensile and compressive properties are the main disadvantages over unidirectional and cross-ply laminates [43]. Hosur et al. [44] observed that the impact response of plain-woven laminates was different to unidirectional laminates due to fibre interlacement, which reduced the delamination initiation. They indicated that bottom layer of the woven laminates did not split during impact loading in comparison to unidirectional laminates. However, splitting in unidirectional laminates initiated the multiple delaminations which could decrease the residual properties. Naik et al. [45] claimed that woven laminates have better impact resistance than unidirectional laminates due to higher transverse strength in woven composites provided by the interlacement of the weft and warp yarns in the preform.

Dehkordi et al. [46] evaluated the impact and CAI response of thermoset composites containing basalt/Nylon hybrid yarns. Their results indicated that hybrid laminates have 41–82% lower compressive strength than the basalt laminates. However, hybrid laminates had higher residual strength with increasing impact energy level. González et al. [47] investigated the drop-weight impact response of hybrid composite laminates made from woven carbon fabric, woven glass fabric and unidirectional carbon tapes. Their results showed that changing the fabric sequence can significantly affected the impact and CAI results as well as the failure mechanisms. They observed that impact energy dissipation decreased when the woven fabrics were used in the mid-plane, and this led to an increase in the residual properties.

Reinforcement architecture also affects the Mode I and Mode II interlaminar fracture toughness whilst 3D and woven laminates have higher fracture toughness than non-crimp laminates due to better delamination resistance [48]. Higher fracture toughness leads to better post impact response in composite laminates [49].

In this study, commingled yarns were produced by mixing E-glass and polypropylene multifilament yarns with varying ratios. E-glass fibres were used as the main reinforcement and a smaller proportion of thermoplastic fibres (PP) were used as the toughening medium. The hybrid yarns were converted into biaxial preforms with the aid of an automated robotic tow placement machine developed at the University of Manchester [50]. Impact behaviour and damage resistance of E-glass/Epoxy non-crimp, E-glass-Polypropylene/Epoxy non-crimp and E-glass-Polypropylene/Epoxy woven composite samples were compared using force-time, force-displacement and energy-time curves; non-destructive evaluation (ultrasonic C-Scanning) and post impact inspection using SEM were performed. Some preliminary CAI results are reported to demonstrate the damage tolerance that can be achieved by commingling of GF with thermoplastic PP fibres.

2. Experimental details

2.1. Commingled yarn processing

The basic material properties of reinforcing yarns provided by the manufacturer are presented in Table 1. E-glass and

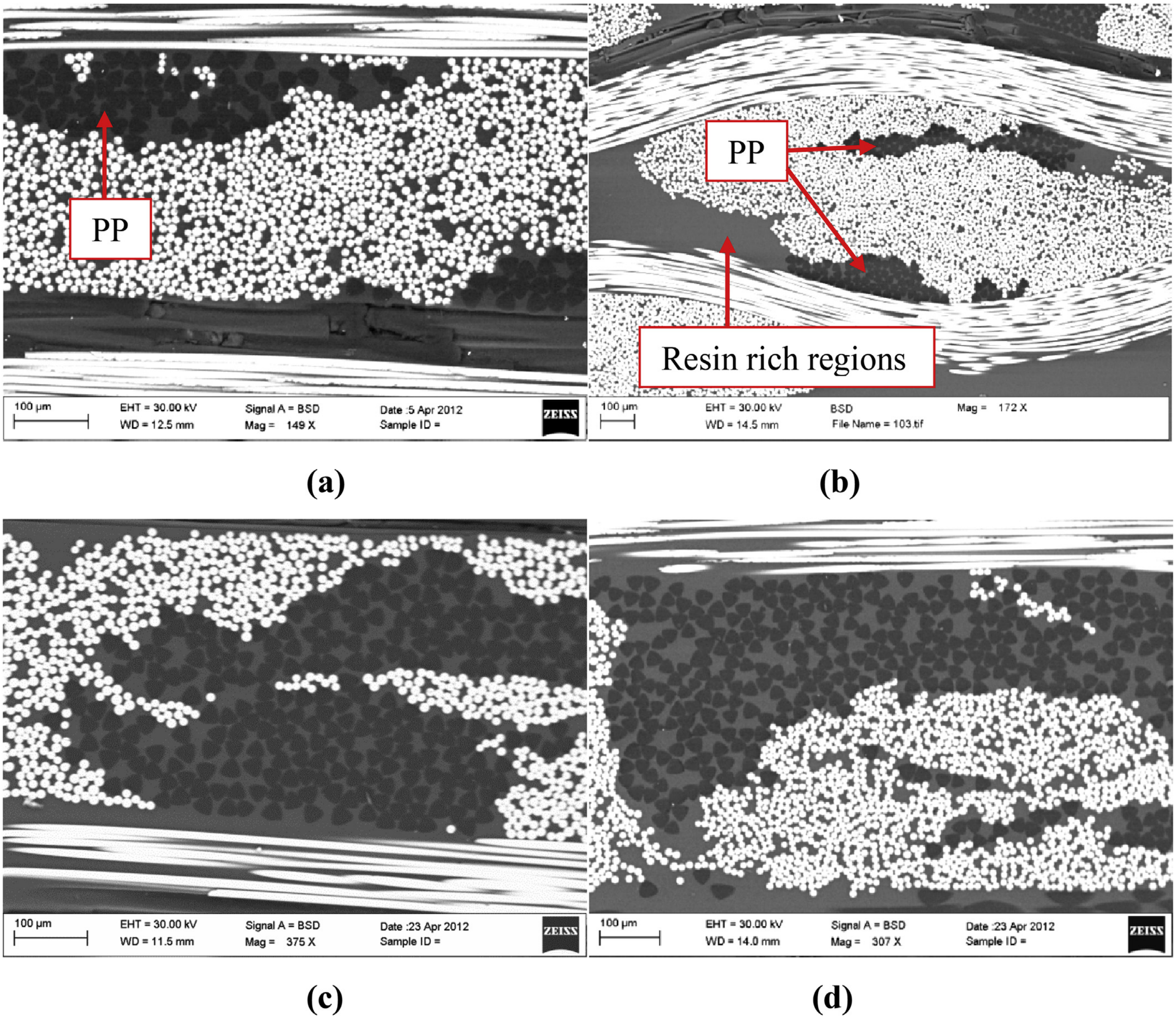

Fig. 6. Final composite laminate cross-sections with different types of commingled yarns: a) 12PPC, b) 12PPW, c) 18PPC and d) 22PPC sample.

Table 5
High energy (500 J) impact test results: Peak force and absorbed energy.

Sample	Force (kN)	Energy (J)	Coupon volume (cm^3)	Specific energy (J/cm^3)
GFC (6 layers)	10.23 (±0.884)	79.6 (±10.0)	10.7	7.4
GFC (10 layers)	16.80 (±1.300)	163.0 (±12.1)	16.6	9.8
GFC (14 layers)	21.5 (±0.398)	246.5 (±6.1)	22.6	10.9
GFC (16 layers)	23.6 (±1.600)	273.1 (±15.0)	25.9	10.5
12PPC	22.2 (±0.875)	269.5 (±5.0)	26.0	10.4
18PPC	23.4 (±0.787)	283.0 (±7.1)	28.6	9.8
22PPC	24.2 (±0.860)	299.9 (±3.5)	32.5	9.2

polypropylene fibres were supplied by PPG Industries [51] and Drake Extrusion [52] respectively.

A commingling nozzle was developed in order to mix the polypropylene fibres with the glass fibre reinforcement as in Fig. 1. There are several air inlets in the commingling nozzle. Air blown at a 45° angle is expected to open the bundles of the yarns as they pass through the nozzle. Other air inlets which are perpendicular to yarn direction are for mixing the opened GF and PP bundles to achieve the final compact yarn structure. Each orifice diameter is 1 mm. The yarn channel is wide enough (4 mm) to accommodate different yarn thicknesses. The nozzle was mounted on a Gemmill&Dunsmore Twisting Fancy Yarn Machine in order to produce final commingled yarns as in Fig. 2.

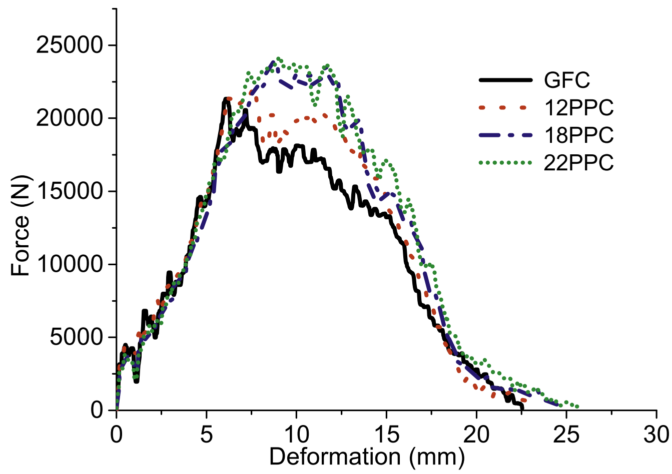

Fig. 7. Force-Deformation history of the samples during high energy impact (500 J).

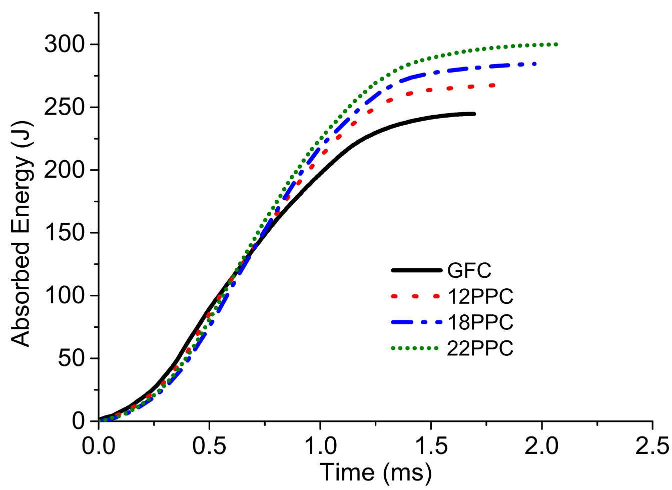

Fig. 8. Absorbed energy-Time history of the non-crimp samples during high energy impact (500 J).

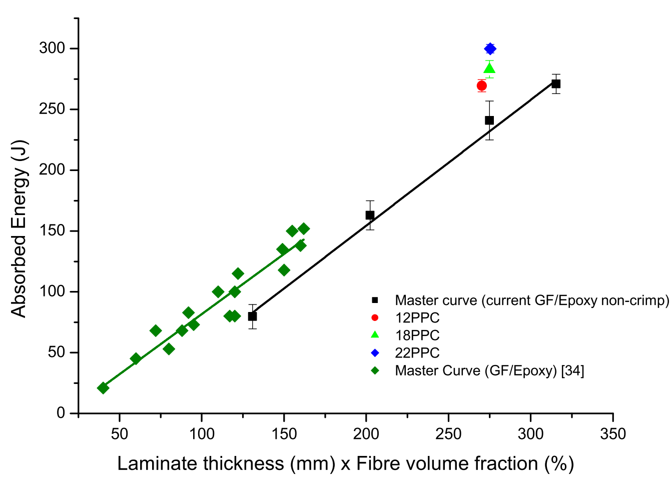

Fig. 9. Absorbed energy as a function of laminate thickness and fibre volume fraction.

After several trials with varying air pressure, 2 bar pressure was found to be optimum for comingling polypropylene and E-glass fibres. Glass and polypropylene filaments are fed into the nozzle with constant yarn tension. Feeding and take up roller speeds influenced the commingled yarn quality with 7% overfeed rate was found to be effective in producing uniform comingling. Glass and polypropylene fibre volume fractions in different commingled yarns are listed in Table 2.

SEM images of yarn cross-sections showing the degree of mixing are presented in Fig. 3 (E-glass fibres appear as white dots and PP fibres appear as black dots). It can be observed that there is some degree of mixing between polypropylene and E-glass yarns. Polypropylene fibres were located at different places, which were in the core or the periphery of the commingled yarn according to the air flow inside the nozzle. Polypropylene yarns are surrounded by E-glass fibres in Fig. 3b while they are within and around E-glass fibres as shown in Fig. 3c.

In traditional thermoplastic composites, commingled process help to reduce void content during heating and consolidation of the polymer composite and hence improved strength. In the present study, these GF/PP commingled yarns have been used in a thermoset resin system. In addition to improved impact performance, inclusion of PP fibres may result in cost and weight reduction since commodity PP fibres have lower density and cost in comparison to glass fibres.

2.2. *Composite laminates with commingled yarns*

Laminates were produced by the placement of commingled yarns on a pinned flat frame using a tow placement machine (at the University of Manchester) as shown in Fig. 4. The tow placement density was fixed at 8 yarns per cm. for the non-crimp preforms. The layer stacking sequence was $[0, 90]_7$. Composite laminates were made by a vacuum bagging method with Araldite LY 564 epoxy resin (75% wt) and Aradur 3486 hardener (25% wt) mixture. Once the resin infusion was completed, the composite samples were heated in the oven at 80 °C for 8 h for curing. Composite laminate panels with E-glass and three different hybrid yarns were produced in a non-crimp configuration. Composition of commingled yarns is presented in Table 2 and the resulting laminate specifications are presented in Table 3.

Plain woven preforms were produced with 20%PP (Table 2) commingled yarns. In the woven fabric, warp and weft densities were 8 yarns per cm. Linear density of the yarn was 633 tex. Final woven composite panels consisted of 7 layers (equivalent to non-crimp preforms) and the identical resin infusion technique was used for the woven fabric laminate (12PPW).

3. Test methods

3.1. *Commingled yarn tests*

Tensile tests were performed according to the ASTM D2256-02 standard test method with 250 mm gauge length. An Evo50 scanning electron microscope (SEM) was used to evaluate the fibre distribution of composite samples at around 30 kv voltage. Fibres were cold moulded before taking the cross-section images by mixture of Araldite 3138 epoxy resin and Araldite 3140 hardener. Moulded samples were ground and polished in order to have clearer images. Carbon coating was applied to the polished samples before observing the images in the SEM. Density and volume fraction of commingled yarns were measured using a Mettler Toledo analytical balance [53] according with ASTM D792 - 08 and BS EN ISO 1172:1999 test methods.

3.2. *Composite specimen tests*

In this work, we included thermoplastic fibre volume as part of matrix volume fraction, since the reinforcement comes primarily

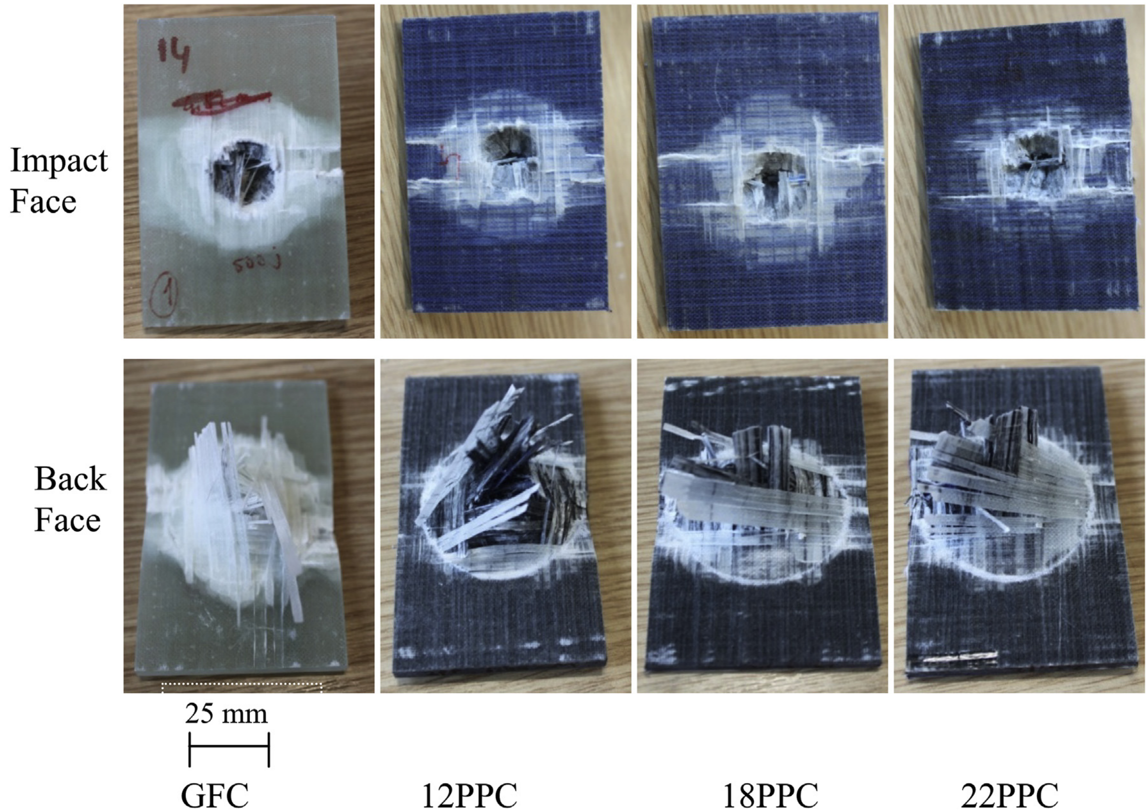

Fig. 10. 500 J impacted samples showing the contact and back faces.

from the glass fibres. Density and volume fraction calculations were calculated in accordance with ASTM D792 - 08 and BS EN ISO 1172:1999 test methods as listed in Table 3. It can be seen that the fibre volume fraction in the woven composite samples (12PPW) is lower than the non-crimp composite samples (12PPC) due to inherent crimp in woven fabrics. Additionally, thickness of the woven composite is slightly higher than non-crimp structure (12PPC) again due to the presence of crimp that prevents perfect nesting. It can also be seen from Table 3 that areal density decreased approximately 8% for 12PPC, 12% for 18PPC, and 16% for 22PPCsamples by the addition of PP fibres.

Test specimens were cut into 89 mm × 55 mm as per the test protocols used by Prichard and Hogg [54]. The samples were subjected to 500 J (high velocity impact) energy using CEAST 9350 drop weight impact machine in this study to measure penetration impact resistance and maximum energy absorption behaviour. The impactor force and mass was 35 kN and 5 kg respectively, with a 20 mm diameter striker.

In addition to the high energy impact test, low energy impact tests were also conducted at 20 J, 30 J, 40 J, and 50 J in order to evaluate the damage resistance. The impactor was automatically arrested after rebounding to avoid a second strike. Once the low energy impacts were completed, the damaged samples were used for CAI tests using an INSTRON 5989 mechanical testing machine with constant displacement of 0.5 mm/min and a 300 kN unit cell. The compressive test fixture (a modification of the Boing test rig) has adjustable retention plates to support the specimen edges and inhibit buckling when the specimen is end-loaded. The same SEM imaging technique was used as for the previous commingled yarn evaluation. Midas-NDT Jet-probe Ultrasonic C-Scan was used to calculate the damage areas after the low velocity impact tests. The Airbus AITM1-0010 test method was used in order to measure dent depth of the composite laminates. Dent depth of laminates was measured on the impacted face right after the impact loading using digital depth gauge.

4. Results and discussions

4.1. Commingled yarn test results

Table 4 presents tensile test results of hybrid comingled yarns with different proportion of polypropylene fibres. Tensile test results for yarn (tensile modulus and strength) were initially obtained in textile units (cN/Tex) but subsequently normalised into engineering units (KPa, MPa) with the aid of solid cross-sectional area of the fibres.

The tensile strength of the hybrid yarns decreased from 1026 MPa (with 0% PP fibres) to 615 MPa (with 35% PP fibres) while the equivalent modulus dropped from 48.7 GPa to 31.2 GPa, respectively with the addition of polypropylene fibres. Fig. 5 shows the truncated stress-strain history of the E-glass, polypropylene and commingled yarns. The breaking strain values are shown until 0.1 mm/mm or 10% since beyond that the strength drops dramatically to that of PP. However, the measured breaking strain values are presented in Table 4 for completeness. It can be seen from the Fig. 4 that there are two breaking points for the hybrid yarns. Yarns (E-glass) with lower elongation and higher stress break first (I) and then breaking of second yarn (polypropylene) happens (II) when the yarns reach their maximum elongation point. It can also be seen that there is a decrease in tensile strain values for commingled yarns compared to100% PP yarn (Table 4).

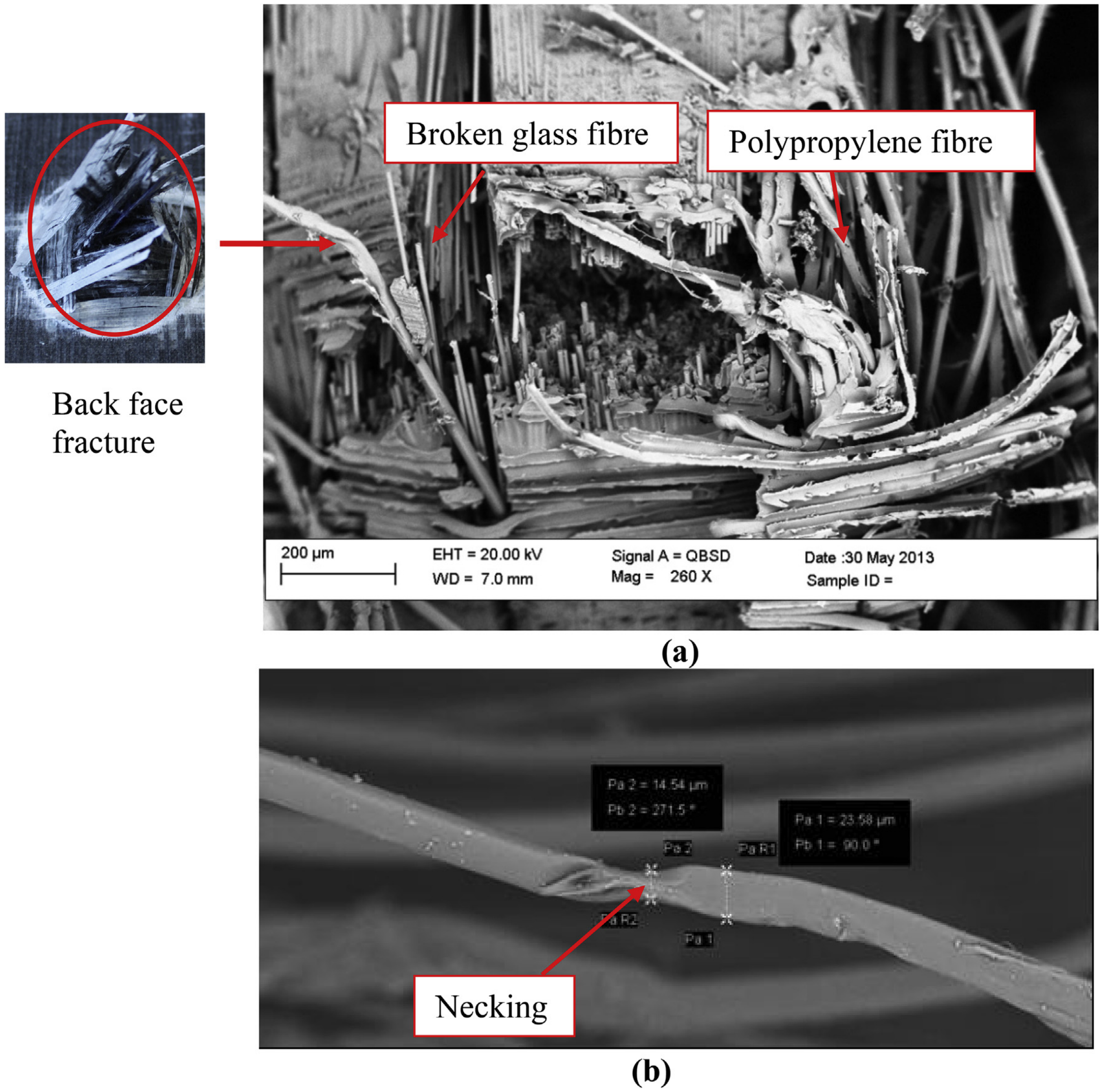

Fig. 11. SEM images of the fully impacted 18PPC sample: a) broken glass fibres, b) polypropylene plastic deformation and necking.

4.2. Composite test results

4.2.1. High velocity impact test results

Fig. 6 shows SEM images of non-impacted $[0/90]_7$ composite samples which consist of different polypropylene ratios. The 18PPC and 22PPC samples showed better mixing when compared to 12PPC suggesting that the fibres mix better with an increasing PP volume fraction. Mixing quality of the yarns is better in non-crimp structures in comparison to woven yarns (12PPW) as fibres tend to segregate due to the rigours of weaving (Fig. 6b).

High impact energy (500 J) test results of non-crimp samples are listed in Table 5 and shown in Figss. 7–8. Glass Fibre Composites (GFCs) consisting of 6–16 layers and hybrid laminates consisting of 14 layers with different proportion of PP fibres were tested at 500 J of impact loading. As it can be seen from results, GFC(14 layers)composite samples absorbed 246 J while hybrid composites with increasing proportion of PP fibres absorbed 270, 283, and 300 J, respectively. Similarly, peak force increased with the increase in proportion of PP fibres (Table 5).

Caprino and Lopresto [55] presented that fibre volume fraction, impactor diameter, and lamina thickness are the main parameters to affect penetration energy of the composite samples. Using the same impactor for all the tests, absorbed energy was plotted against the product of laminate thickness and fibre volume fraction (Fig. 9), and the results were compared with those presented by Babic et al. [56]. Absorbed energy values for GFC samples with various number of layer (and hence thickness) fall on a straight line (similar to that of Babic et al.); these values for hybrid laminates fall above the master curve with the highest value for the laminate with 22% PP. Table 5 also presented energy absorption values normalised to coupon volume. Normalised or specific energy values increased slightly with stack thickness of glass fibre laminates. However, glass-pp hybrid laminates have comparable specific energy absorption values in spite of having lower glass fibre volume fractions. PP fibres appear to make significant contribution under dynamic loading whereas they make negligible contribution under static loading.

It is important to understand the mechanisms involved in energy absorption during high energy impacts that result in full

Table 6
Low impact energy (20–50 J) test results.

Impact energy (J)	Peak force (N)	Peak deformation (mm)	Absorbed energy (J)
20J			
GFC	8408 (±96)	3.92 (±0.28)	12.13 (±0.60)
12PPC	7968 (±76)	3.94 (±0.10)	12.74 (±0.10)
18PPC	7976 (±60)	4.03 (±0.10)	12.74 (±0.15)
22PPC	8064 (±120)	3.98 (±0.11)	12.52 (±0.10)
12PPW	9019 (±400)	3.63 (±0.20)	10.33 (±0.90)
30J			
GFC	10393 (±75)	4.90 (±0.03)	20.73 (±0.65)
12PPC	10213 (±141)	5.14 (±0.11)	21.62 (±0.20)
18PPC	10483 (±192)	5.18 (±0.10)	21.47 (±0.68)
22PPC	10609 (±71)	5.22 (±0.10)	21.05 (±0.35)
12PPW	10925 (±182)	4.52 (±0.10)	16.41 (±0.55)
40J			
GFC	12712 (±316)	5.70 (±0.13)	26.86 (±0.24)
12PPC	12911 (±60)	5.83 (±0.10)	26.94 (±0.33)
18PPC	12280 (±184)	5.91 (±0.10)	27.16 (±0.32)
22PPC	12976 (±282)	5.89 (±0.10)	27.00 (±0.52)
12PPW	12779 (±225)	5.32 (±0.10)	23.02 (±0.64)
50J			
GFC	14778 (±164)	6.31 (±0.10)	32.95 (±0.55)
12PPC	14789 (±179)	6.53 (±0.10)	33.72 (±1.21)
18PPC	15119 (±87)	6.40 (±0.13)	33.24 (±0.51)
22PPC	14930 (±127)	6.54 (±0.10)	33.74 (±1.09)
12PPW	13358 (±338)	5.74 (±0.11)	30.72 (±1.28)

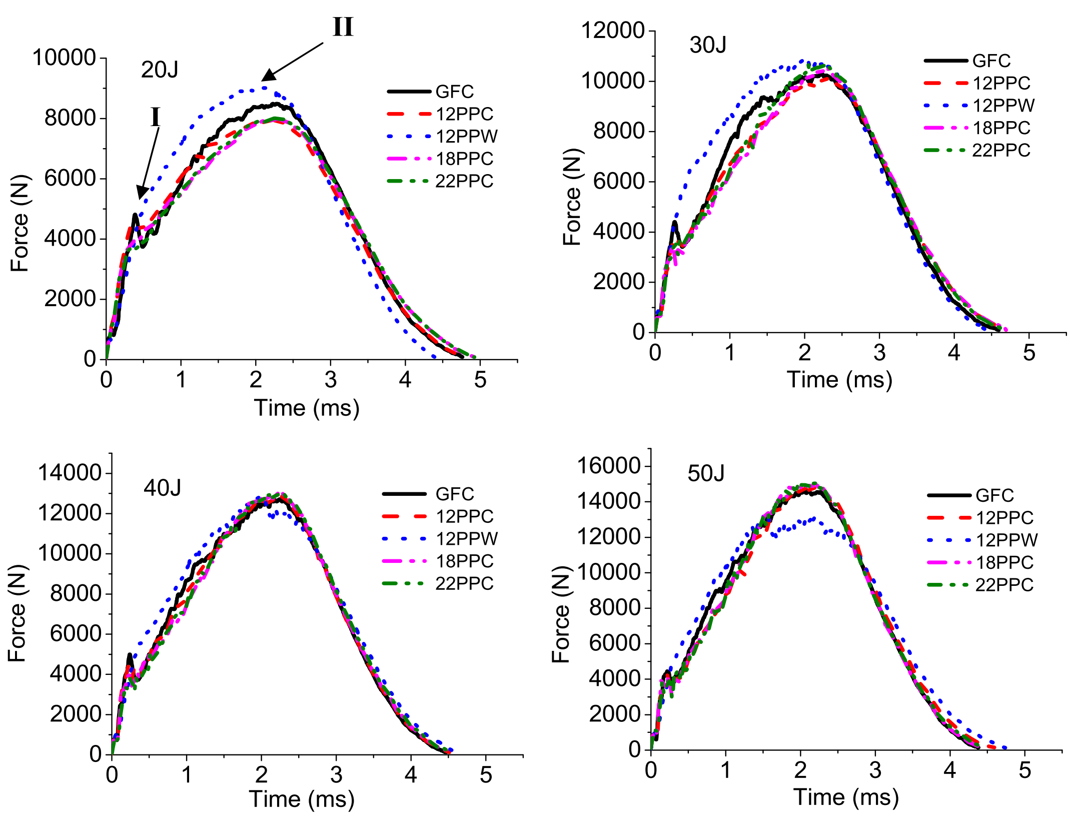

Fig. 12. Force-time history of the samples at different impact energy levels (20–50 J).

penetration (Fig. 10). Schrauwen [41] pointed that the penetration energy is primarily due to the fibre fracture. Peak force as well as the absorbed energy (Table 5) increase with the proportion of PP fibres (and a corresponding reduction in glass fibre volume fraction) clearly indicating the role of thermoplastic fibres in high energy impact loading. Fig. 7 shows that the hybrid laminates produce higher penetration forces as well as sustain this peak force for a much longer duration, resulting in a larger area under force-deformation curve. Glass fibres appear to play a dominant role for energy absorption initially (Fig. 8), due to higher modulus and lower strain to failure, and the PP fibres appear to start contributing from 1 ms onwards. SEM images (Fig. 11) appear to corroborate the fact that PP fibres undergo extensive plastic deformation and necking prior to failure. In fact, in hybrid laminates, weak interface

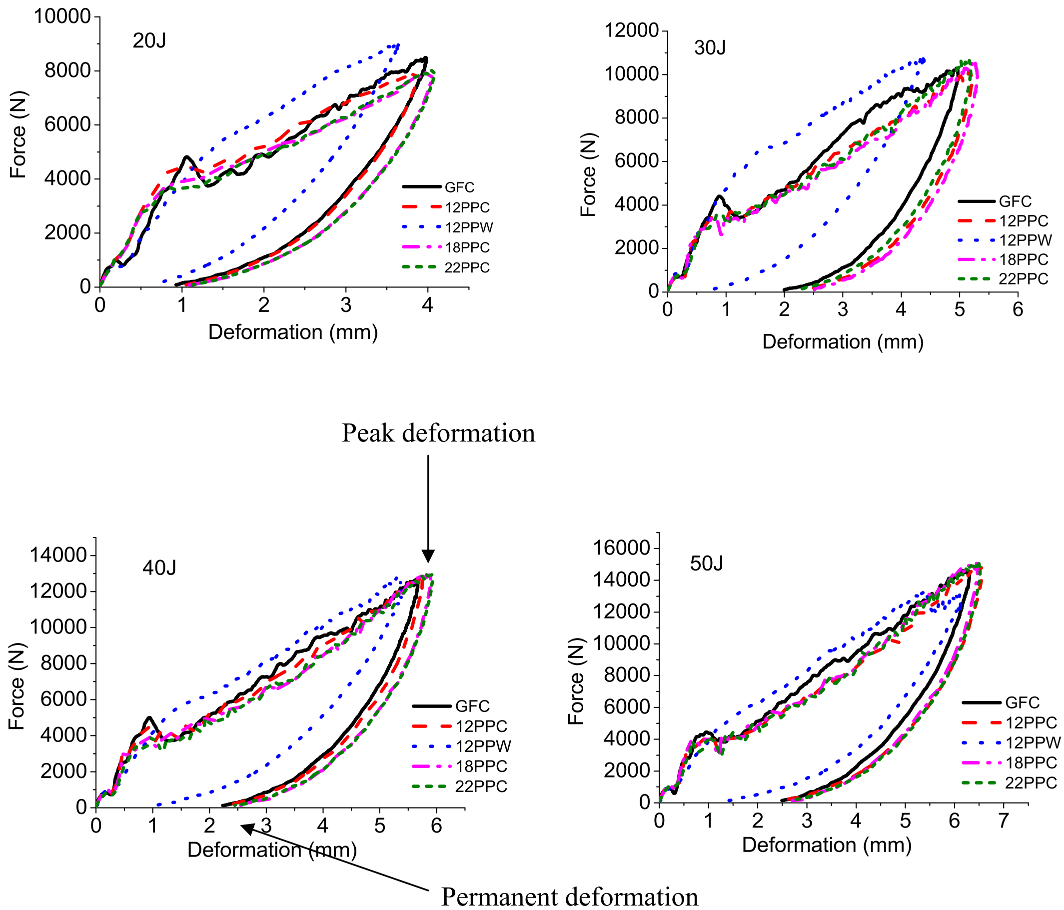

Fig. 13. Force-deformation history of the samples at different impact energy levels (20–50 J).

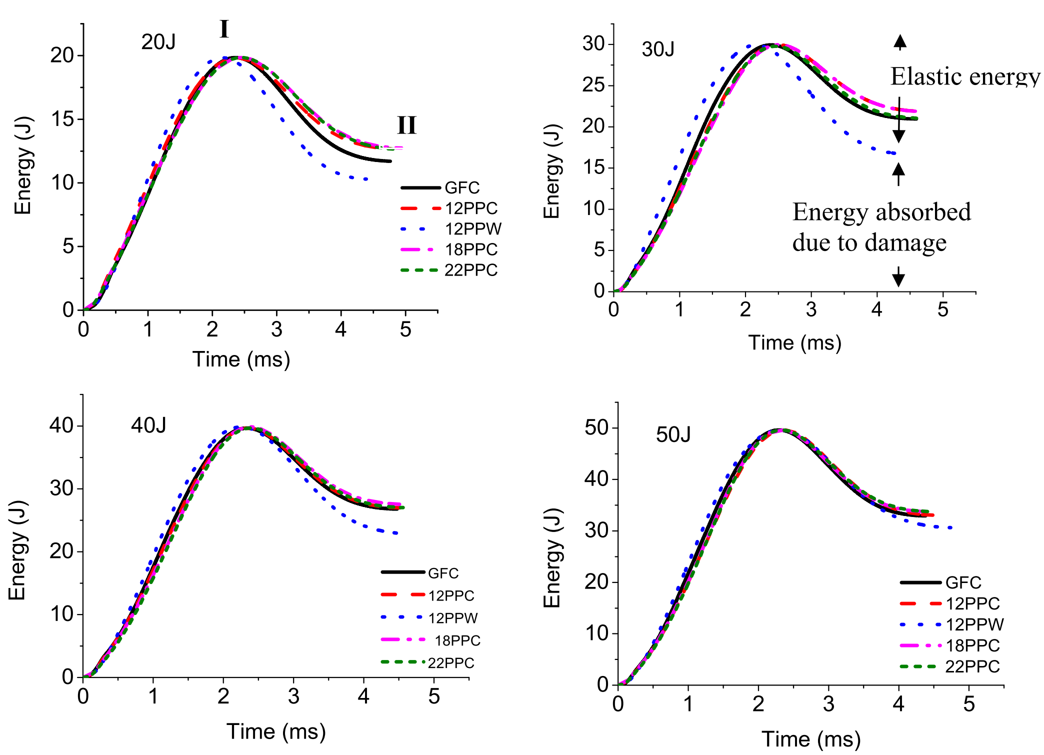

Fig. 14. Energy-time history of the samples at different impact energy levels (20–50 J).

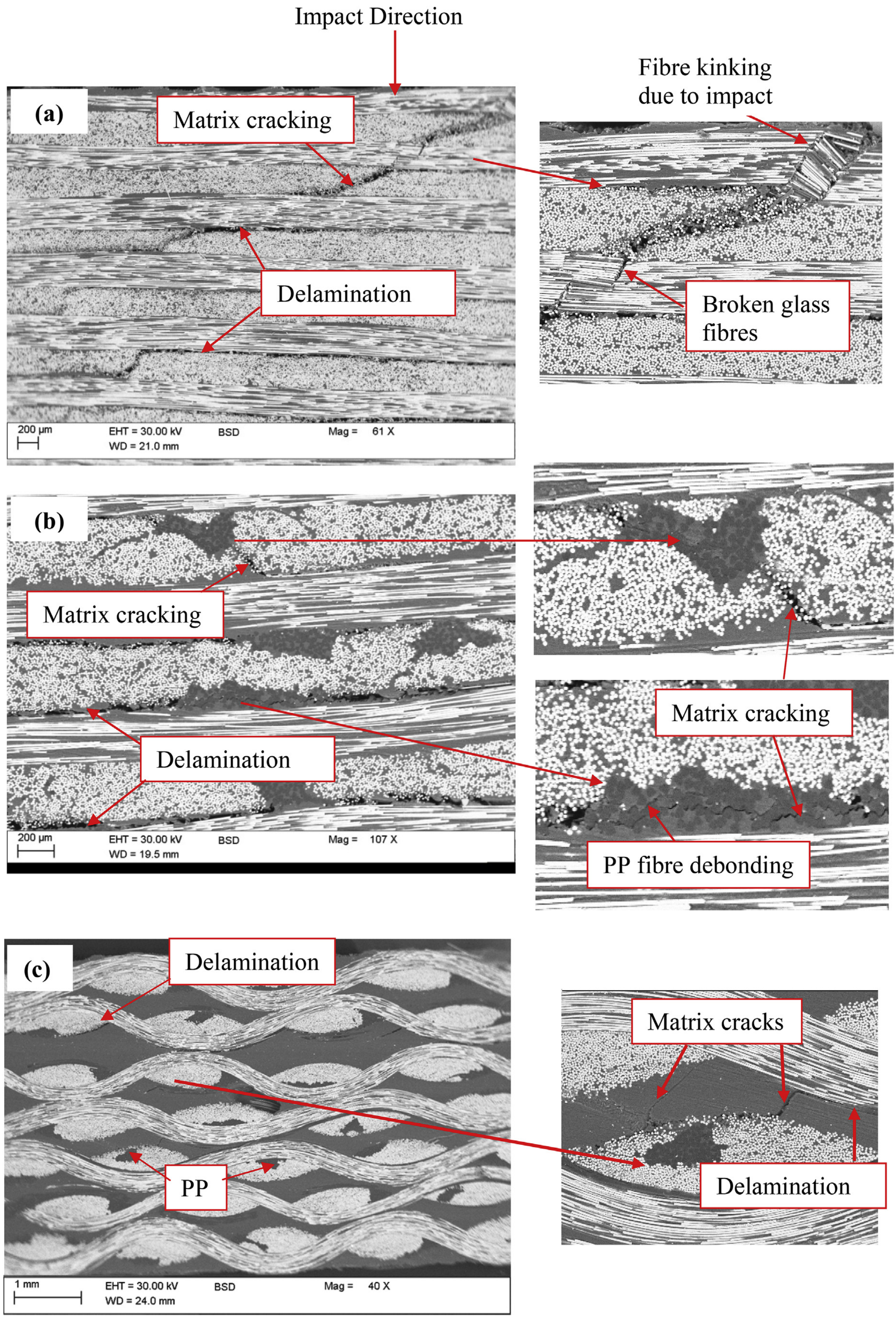

Fig. 15. Cross-section images of 20 J impact:a) GFC, b) 12PPC and c) 12PPW sample.

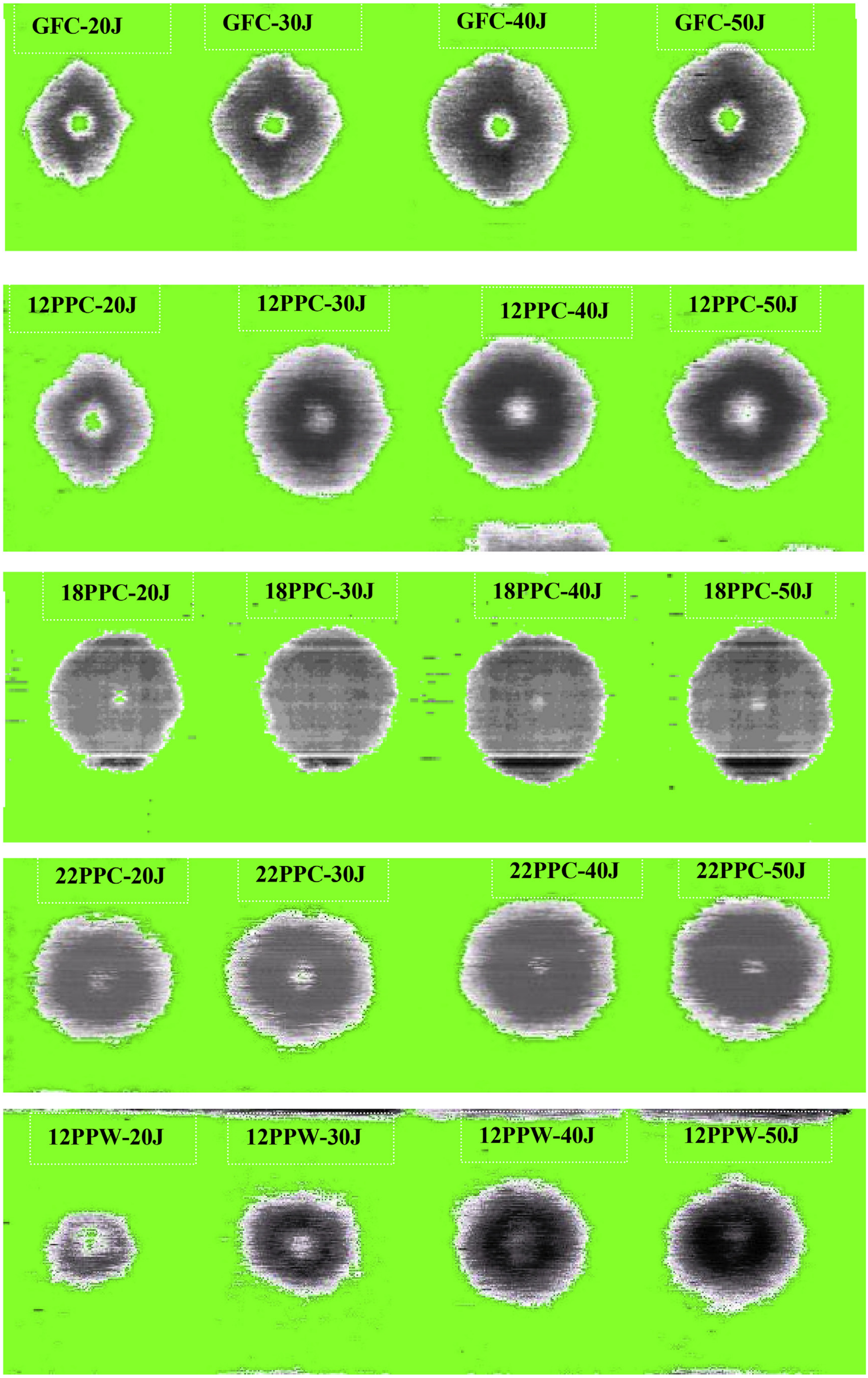

Fig. 16. C-Scan images of woven and non-crimp samples after different impact energy levels.

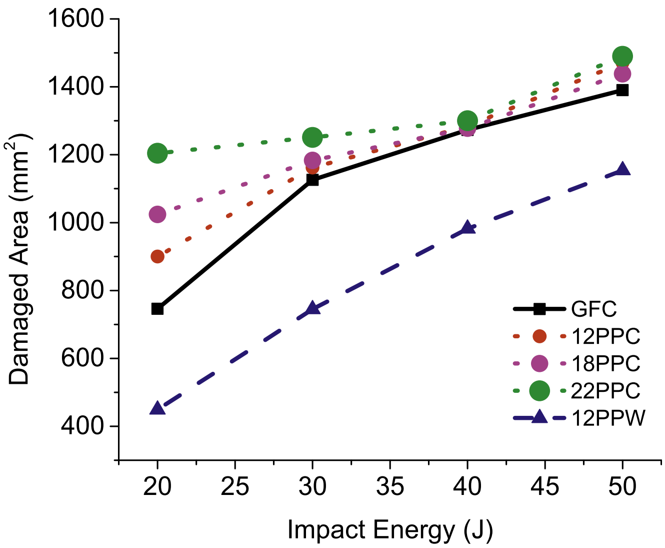

Fig. 17. Damage areas of woven and non-crimp samples after different impact energy.

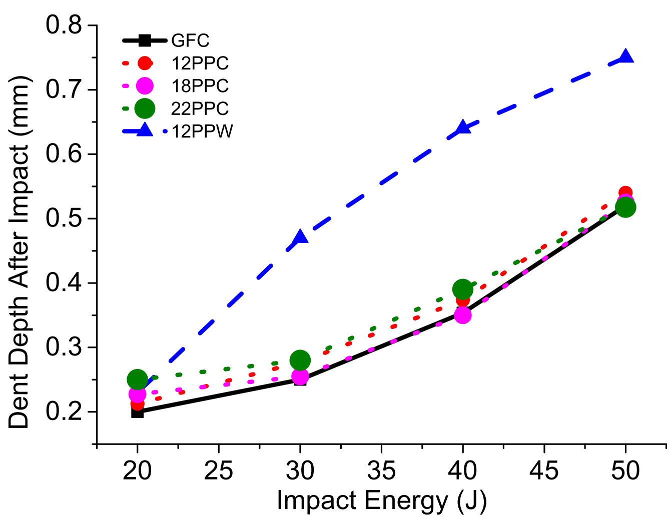

Fig. 18. Dent depth versus impact energy response of different samples.

between PP fibres and the matrix promote debonding beyond the impacted region, resulting in a larger 'fibre net' to participate in the stretching mode of deformation. Additionally, stretching reduces PP fibre diameter resulting in debonding. Peak force is sustained for a longer duration (Fig. 7) due to this thermoplastic fibre network extending deep into the laminate.

4.2.2. Low velocity impact test results

Low velocity of low energy impact tests were conducted on both glass and hybrid laminates in the range of 20–50 J of impact energy. At these energy levels, impactor did not fully penetrate the samples and a proportion of impact energy was stored as elastic energy; this elastic energy was transferred back to the impactor causing it to rebound. Peak force, peak deformation and absorbed energy values increased with impact energy levels (Table 6); however the difference between GFC and PPC hybrid samples was marginal.

Figs. 12 and 13 present force-time and force-deformation graphs respectively for various laminates impacted at 20–50 J. Non-crimp laminates exhibit a distinct peak (I) after 4000 N; GFC samples exhibit a sharp peak while the PPC hybrid laminates exhibit a blunt peak. On the other hand, woven laminates exhibit a smooth curve with higher peak loads and correspondingly lower deformations in comparison to non-crimp laminates. Woven laminates have also exhibited smallest plastic deformation (Fig. 13) whereas all non-crimp laminates exhibit similar level of plastic deformation; however, at 50 J, impact energy absorption in woven laminates is similar to non-crimp laminates and a corresponding drop in peak loads (Fig. 14).

Fig. 15 shows SEM images of the samples subjected to 20 J impact, for Glass/epoxy (GFC) and Glass-PP/Epoxy (12PPC and 12PPW) samples. Extensive fibre/tow breakages, matrix cracks and delamination can be seen in pure glass epoxy samples (GFC), Fig. 15a, with compressive failure at the top layer. In the case of samples with PP (12PPC), there are extensive matrix cracks and delamination but not fibre/tow breakages (Fig. 15b). It appears that PP fibres have a cushioning effect and hence protect glass fibres from impact damage. Impact energy is absorbed mainly by delamination and matrix cracks. Woven samples (12PPW) with PP exhibited mainly matrix cracks and significantly lower delamination in comparison to 12PPC. Again, woven samples did not show any significant fibre/tow breakages (Fig. 15c). Due to interlacement and crimp, delamination is suppressed in comparison to bi-directional non-crimp architectures.

It is clear that damage area increases with increasing of impact energy as in C-Scan images shown in Figs. 16–17. For each impact energy level, damage area increased slightly with % PP fibres, with this effect more clearly visible at lower energy levels. Woven laminates have significantly lower damage areas and a higher dent depth in comparison to non-crimp laminates (Fig. 18). It was observed that impact damage was spread over a larger area in non-crimp laminate whereas they were mostly localised in the woven samples to promote higher dent depths. Those bigger dent depths in the woven laminate may be attributed to a) lower bending stiffness due to tow crimp, b) impact energy is absorbed by a smaller area resulting in greater plasticity/stiffness degradation and more localised damage under the impactor. Larger dent depth along with smaller damage area in woven laminates may be advantageous in identifying and repairing the damage [57].

4.2.3. Impact damage mechanisms

It is important to compare the damage mechanisms in GFC laminates with glass-PP hybrid laminates. Due to the very nature of impact loading, it is not possible to capture the damage sequence with current experimental techniques. SEM images (Fig. 15) along with force-time or force-deformation graphs (Fig. 19) during impact loading may be used for interpreting the damage mechanisms. Fig. 15a shows, at 20 J impact loading, clear large area interply delaminations in GFC laminates, matrix cracks through plies and broken glass fibre tows. Broken glass tows may be due to shock loading or kink-band formation in the compression region. Hybrid laminates (12PPC) show tortuous delamination paths running close to PP fibres due to relatively poor interface between PP fibres and the matrix. In woven laminates, matrix cracks and highly localised delaminations have been observed. Interlacing architecture in woven laminates seems to inhibit intra-tow crack growth; tortuous sinusoidal interface between fabric layers may also be responsible for smaller interlaminar crack growths in woven laminates. Extensive fibre damage, found in GFC laminates, is not visible in both cross-ply and woven hybrid laminates. PP fibres appear to cushion the impact loading on glass fibres and appear to diffuse the impact energy, perhaps through extensive intra-tow debonds (yet to be verified through better imaging techniques).

Fig. 19 reveals some interesting observations. During 20 J impact loading (Fig. 19b–c), GFC laminates experience a sharp peak around 5 kN load whereas the hybrid laminates experience a blunt and

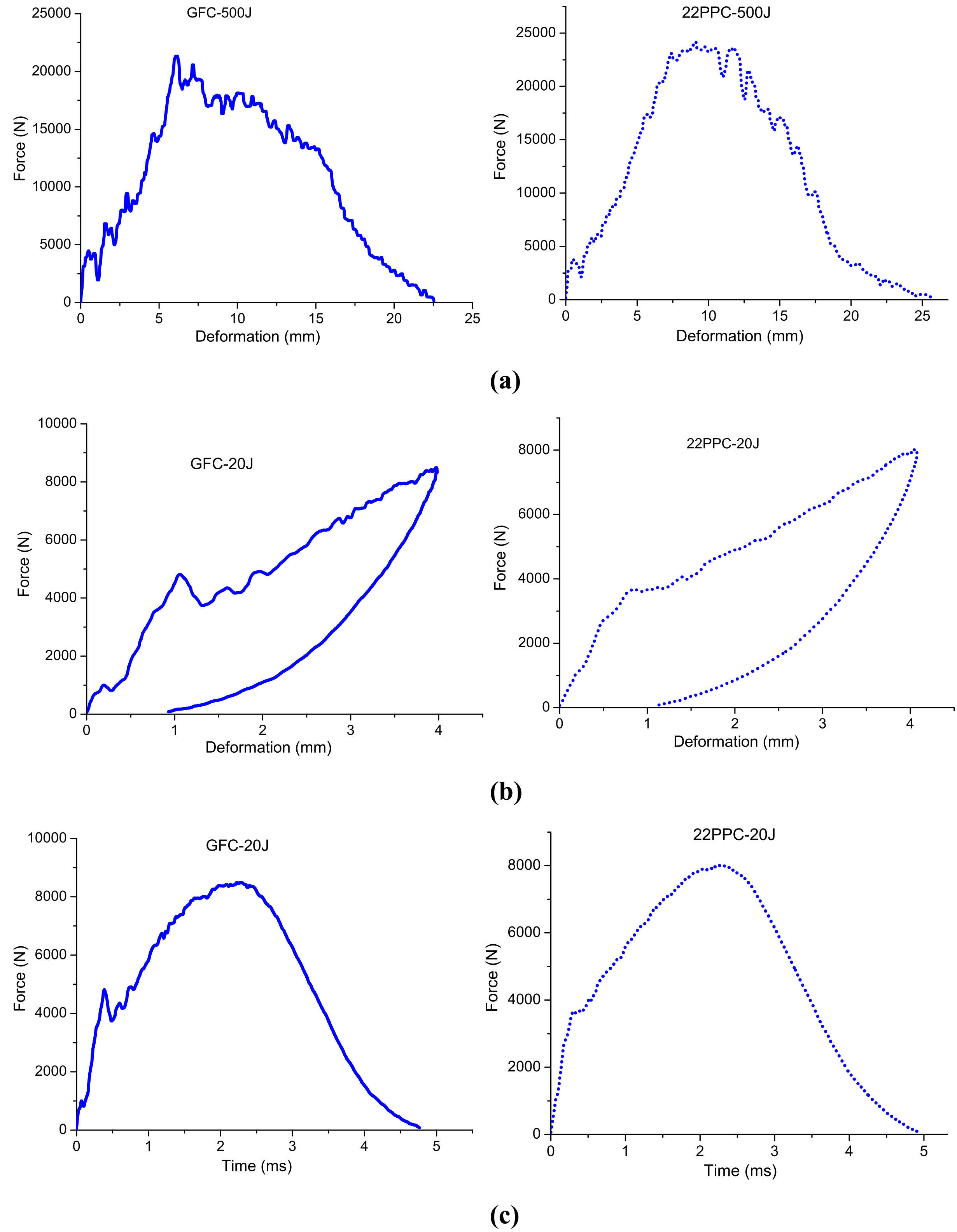

Fig. 19. Impact behaviour of GFC and 22PPC samples: a) force-deformation history at 500 J, b) force-deformation history at 20 J, and c) force-time history at 20 J.

subtle peak around 4 kN. GFC laminates may be experiencing a major damage event such as tow failure or extensive delamination; whereas hybrid laminates experience more diffused and gradual damage due to tortuous damage path.

During 500 J impact loading, several peaks can be observed in force-deformation curve for GFC laminate whereas hybrid laminates one peak at around 4 kN, less intense than GFC. Once the force-deformation curve reaches the peak load, hybrid laminates

Table 7
Compression and CAI (20 J impact energy) strength of the non-crimp and woven samples.

Sample	Compression modulus (GPa)	Compression strength (MPa)	CAI strength (MPa)	Normalised compression modulus (GPa)	Normalised compression strength (MPa)	Normalised CAI strength (MPa)
GFC	17.9 (±0.31)	298.5 (±10)	134.5 (±8.2)	17.9	298.5	134.5
12PPC	15.5 (±0.35)	233.4 (±16)	115.0 (±3.5)	16.9	254.1	125.2
18PPC	13.9 (±0.27)	191.0 (±18)	101.2 (±4.0)	15.7	216.9	114.9
22PPC	11.6 (±0.29)	149.6 (±7.3)	90.5 (±4.5)	13.8	178.9	108.2
12PPW	10.8 (±0.30)	111.6 (±4.0)	92.7 (±3.5)	12.3	128.0	95.3

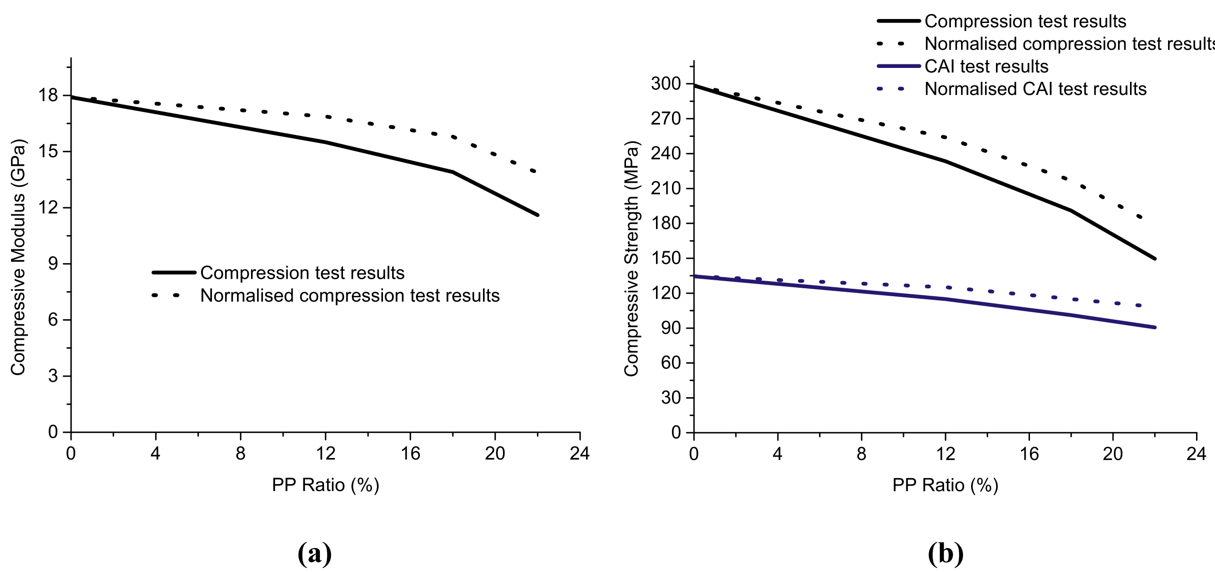

Fig. 20. Normalised (density) for: a) compression modulus and b) compression strength of non-crimp laminates with different PP ratios.

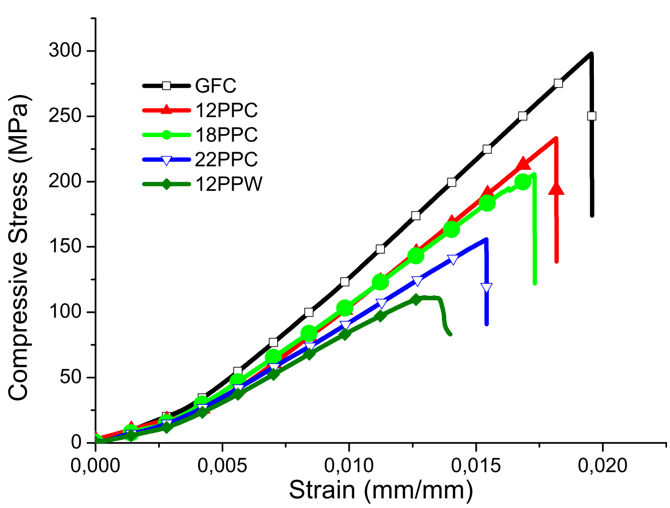

Fig. 21. Stress-strain curves of laminates during compressive loading.

appear to hold this peak load for several mm of deflection in comparison to instantaneous drop in load for GFC. It appears that the PP fibres undergo plastic deformation and offer significant resistance during penetration through the bottom skin.

4.2.4. Compression and CAI test results

Table 7 and Fig. 20 present compression and Compression After Impact (CAI) results, at 20 J impact, for laminates with various levels of PP fibres. The results have also been normalised to material density. It can be seen that compression strength and modulus, before and after impact, decrease with increase in %PP fibres due to corresponding reduction in the load-bearing glass fibre volume fraction. It may be observed from the graphs (Fig. 20) that there is a linear reduction in compressional properties up to about 18% PP, and steeper reduction after this value indicating potential limits to the degree of hybridisation.

Comparing density-normalised properties of 18PPC with GFC (Table 7), there is a 12% reduction in compression modulus and 28% reduction in compression strength due to hybridisation with 18% PP fibres. However, reduction in compression strength after impact (CAI) is less dramatic with 14% reduction in CAI values due to the presence of 18% PP fibres. This is probably due to the fact that hybrid laminates exhibit less fibre damage due to the cushioning effect of PP fibres and retain a greater proportion of strength after impact (45% for GFC vs 53% for 18PPC). Additionally, hybrid laminates (PPC) exhibit diffused intra-tow damage through PP fibres in comparison to planar inter-laminar cracks in GFC laminates. As a result, GFCs are more prone to buckling during a CAI test.

In woven samples with PP (12PPW) undamaged compression strength is significantly lower than cross-ply laminate with similar amount of PP fibres as shown in Fig. 21. This can be attributed to crimp in woven samples. However, the residual compression strength as a percentage of undamaged samples is significantly higher in woven samples (83%) in comparison to cross-ply laminate 12PPC (50%). This is due to smaller delaminated regions (Fig. 15c) and damage areas (Fig. 16) are formed at 20 J impact energy, indicating that 12PPW laminate is more impact damage resistant (less delamination) and damage tolerant (higher residual compressive strength) than the equivalent non-crimp laminates. Intra-tow fracture toughness (G_{Ic} and G_{IIc}) is likely to be higher in woven laminates due to the presence of interlacement, and inter-ply fracture toughness is likely to be higher due to non-planar wavy interface between the plies due to tow crimp. Undamaged compression strength of woven laminates may be improved by changing the weave geometry, for example by keeping majority of tows un-crimped with a small number of finer tows interlacing the entire laminate (3D weaves).

5. Conclusions

Tow-level hybridisation of glass fibres with commodity polypropylene fibres (PP), with relatively weak interface to the thermoset matrix, resulted in interesting damage mechanisms with potential for improved damage tolerance. Glass fibre composites (GFC) exhibited clear delaminations between the plies, matrix transverse cracks within plies and significant fibre damage at relatively low impact energies. In the case of glass-PP hybrid laminates, delaminations are more diffused and tortuous running through PP fibres. In this process of diffused damage, hybrid laminates have a slightly higher damage area but somehow protect the reinforcing fibres from damage. As a result, residual compression strength (as a percentages of undamaged compression strength) is higher for hybrid laminates.

Woven hybrid laminates due to tow interlacements have significantly lower damage area and hence retain higher residual compression strength in comparison to UD cross ply laminates. However, the woven laminates have lower undamaged compression strength due to the presence of fibre crimp. This presents an interesting challenge in designing woven laminates with interlacements but significantly lower crimp.

Analogous to sandwich construction that offers potential for weight reduction in structures subjected primarily to bending loads, tow-scale hybridisation with PP fibres offers similar potential for weight reduction in the case designing for impact loading.

Acknowledgement

This project has been carried under the EPSRC Centre for Innovative Manufacturing in Composites multi-functional multi-material project (grant number: EP/IO33513/1). Erdem Selver is sponsored by the Ministry of National Education of Turkey gratefully acknowledged. The authors acknowledge Mr. Alvaro Silva-Caballero for producing samples with the tow placement machine. The authors also would like to thank PPG Industries and Drake Extrusion LTD for donating glass and polypropylene yarns.

References

[1] Larsson F. Damage tolerance of a stitched Carbon/epoxy Laminate. Compos Part A-Appl S 1997;28(11):923–34.
[2] Administration FA. Pilot's handbook of aeronautical knowledge. Washington: Skyhorse; 2009.
[3] Shi Y, Swait T, Soutis C. Modelling damage evolution in composite laminates subjected to low velocity impact. Compos Struct 2012;94(9):2902–13.
[4] Hawyes VJ, Curtis PT, Soutis C. Effect of impact damage on the compressive response of composite laminates. Compos Part A-Appl S 2001;32(9):1263–70.
[5] Christoforou A, Yigit A, Cantwell W, Yang F. Impact response characterization in composite plates-experimental validation. Appl Compos Mater 17(5): 463–472.
[6] Soutis C, Curtis PT. Prediction of the post-impact compressive strength of CFRP laminated composites. Compos Sci Technol 1996;56(6):677–84.
[7] Mines RAW, Roach AM, Jones N. High velocity perforation behaviour of polymer composite laminates. Int J Impact Eng 1999;22(6):561–88.
[8] Brown K, Brooks R, Warrior N. Characterizing the strain rate sensitivity of the tensile mechanical properties of a thermoplastic composite. Jom-J Min Met Mat S 2009;61(1):43–6.
[9] Chang IY, Lees JK. Recent development in thermoplastic composites: a review of matrix systems and processing methods. J Thermoplast Compos 1988;1(3): 277–96.
[10] Lee RJ. Compression strength of aligned carbon fibre-reinforced thermoplastic laminates. Composites 1987;18(1):35–9.
[11] Vieille B, Casado VM, Bouvet C. About the impact behavior of woven-ply carbon fiber-reinforced thermoplastic- and thermosetting-composites: a comparative study. Compos Struct 2013;101(0):9–21.
[12] Hufenbach W, Böhm R, Thieme M, Winkler A, Mäder E, Rausch J, et al. Polypropylene/glass fibre 3D-textile reinforced composites for automotive applications. Mater Desig 2011;32(3):1468–76.
[13] Bernet N, Michaud V, Bourban PE, Månson JAE. Commingled yarn composites for rapid processing of complex shapes. Compos Part A-Appl S 2001;32(11): 1613–26.
[14] Wakeman MD, Cain TA, Rudd CD, Brooks R, Long AC. Compression moulding of glass and polypropylene composites for optimised macro- and micro-mechanical properties-1 commingled glass and polypropylene. Compos Sci Technol 1998;58(12):1879–98.
[15] Trudel-Boucher D, Fisa B, Denault J, Gagnon P. Experimental investigation of stamp forming of unconsolidated commingled E-glass/polypropylene fabrics. Compos Sci Technol 2006;66(3–4):555–70.
[16] Mazumdar S. Composites manufacturing: materials, product, and process engineering. Florida: CRC Press; 2001.
[17] Woods D, Hine P, Ward I. The impact properties of hybrid composites reinforced with high-modulus polyethylene fibres and glass fibres. Compos Sci Technol 1994;52(3):397–405.
[18] Lee Y-S, Kang K-H, Park O. Response of hybrid laminated composite plates under low-velocity impact. ComputStruct 1997;65(6):965–74.
[19] Park R, Jang J. The effects of hybridization on the mechanical performance of aramid/polyethylene intraply fabric composites. Compos Sci Technol 1998;58(10):1621–8.
[20] Jang J, Moon S-I. Impact behavior of carbon fiber/ultra-high modulus polyethylene fiber hybrid composites. Polym Compos 1995;16(4):325–9.
[21] Miao M, Yan Lai H, Kwok Po Stephen C. Commingling self-twist yarn with filaments1. Text Res J 1994;64(10):563–9.
[22] Kang BC, Min KH, Lee YH, Hwang BB, Herath CN. Microscopic evaluation of commingling-hybrid yarns. Mater Sci Forum 2007;539–543:992–6.
[23] Alagirusamy R, Ogale V, Bhowmick M. Air flow behaviour in commingling nozzles and their influence on properties of commingled yarns. Indian J Fibre Text 2007;32:410–20.
[24] Golzar M, Brunig H, Mader E. Commingled hybrid yarn diameter ratio in continuous fiber-reinforced thermoplastic composites. J Thermoplast Compos 2007;20(1):17–26.
[25] Kang BC, Herath CN, Park JK, Roh YH. An air texturing process for hybridization of different reinforcement filament yarns by commingling process. Mater Sci Forum 2006;532–533:333–6.
[26] Alagirusamy R. Development and characterization of GF/PET, GF/Nylon, and GF/PP commingled yarns for thermoplastic composites. J Thermoplast Compos 2005;18(3):269–85.
[27] Ye L, Friedrich K, Kastel J, Mai Y-W. Consolidation of unidirectional CF/PEEK composites from commingled yarn prepreg. Compos Sci Technol 1995;54(4): 349–58.
[28] Alagirusamy R, Fangueiro R, Ogale V, Padaki N. Hybrid yarns and textile preforming for thermoplastic composites. Text Prog 2006;38(4):1–71.
[29] Thomanny UI, Ermanni P. The Influence of yarn structure and processing conditions on the laminate quality of stampformed carbon and thermoplastic polymer fiber commingled yarns. J Thermoplast Compos 2004;17(3):259–83.
[30] Mader E, Rausch J, Schmidt N. Commingled yarns-processing aspects and tailored surfaces of polypropylene/glass composites. Compos Part A-Appl S 2008;39(4):612–23.
[31] Hogg PJ. Toughening of thermosetting composites with thermoplastic fibres. Mat Sci Eng A-Struct 2005;412(1–2):97–103.
[32] Jang BZ, Chen LC, Hwang LR, Hawkes JE, Zee RH. The response of fibrous composites to impact loading. Polym Compos 1990;11(3):144–57.
[33] Dutra RCL, Soares BG, Campos EA, Silva JLG. Hybrid composites based on polypropylene and carbon fiber and epoxy matrix. Polymer 2000;41(10): 3841–9.
[34] Thanomsilp C, Hogg PJ. Penetration impact resistance of hybrid composites based on commingled yarn fabrics. Compos Sci Technol 2003;63(3–4): 467–82.
[35] Poon C, Benak T, Gould R. Assessment of impact damage in toughened resin composites. TheorApplFractMec 1990;13(2):81–97.
[36] Khondker OA, Leong KH, Herszberg I, Hamada H. Impact and compression-after-impact performance of weft-knitted glass textile composites. Compos Part A-Appl S 2005;36(5):638–48.
[37] Potluri P, Hogg P, Arshad M, Jetavat D, Jamshidi P. Influence of fibre architecture on impact damage tolerance in 3D woven composites. Appl Compos Mater 2012;19(5):799–812.
[38] Atas C, Sayman O. An overall view on impact response of woven fabric composite plates. Compos Struct 2008;82(3):336–45.
[39] Mili F, Necib B. Impact behavior of cross-ply laminated composite plates under low velocities. Compos Struct 2001;51(3):237–44.
[40] Aktas M, Atas C, İçten BM, Karakuzu R. An experimental investigation of the impact response of composite laminates. Compos Struct 2009;87(4): 307–13.
[41] Schrauwen B, Peijs T. Influence of matrix ductility and fibre architecture on the repeated impact response of glass-fibre-reinforced laminated composites. Appl Compos Mater 2002;9(6):331–52.

[42] Bibo GA, Hogg PJ. The role of reinforcement architecture on impact damage mechanisms and post-impact compression behaviour. J Mater Sci 1996;31(5):1115–37.

[43] Kim J-K, Sham M-L. Impact and delamination failure of woven-fabric composites. Compos Sci Technol 2000;60:745–61.

[44] Hosur MV, Adbullah M, Jeelani S. Studies on the low-velocity impact response of woven hybrid composites. Compos Struct 2005;67(3):253–62.

[45] Naik NK, Chandra Sekher Y, Meduri S. Damage in woven-fabric composites subjected to low-velocity impact. Compos Sci Technol 2000;60:731–44.

[46] Tehrani Dehkordi M, Nosraty H, Shokrieh MM, Minak G, Ghelli D. The influence of hybridization on impact damage behavior and residual compression strength of intraply basalt/nylon hybrid composites. Mater Desig.43(0):283–290.

[47] Gonzalez EV, Maimi P, Sainz de Aja JR, Cruz P, Camanho PP. Effects of interply hybridization on the damage resistance and tolerance of composite laminates. Compos Struct 108:319–331.

[48] Boisse P. Composite reinforcements for optimum performance. Cambridge: Elsevier Science; 2011. p. 175–84.

[49] Cantwell WJ, Morton J. The impact resistance of composite materials — a review. Composites 1991;22(5):347–62.

[50] Silva-Caballero A, Potluri P, Jetavat D, Kennon R. Robotic dry fibre placement of 3D preforms. In: Proceedings of 19th international conference on composite materials (ICCM19). Montreal; 2013. p. 639–47.

[51] PPG. http://www.ppg.com/corporate/ppgwind/products/Pages/HYBON.aspx. 2013.

[52] Drake E. http://www.drakeextrusionuk.com/. 2013.

[53] Toledo M. http://uk.mt.com/gb/en/home/products/Laboratory_Weighing_Solutions/Analytical/XPE_Analytical_Balance.html. 2014.

[54] Prichard JC, Hogg PJ. The role of impact damage in post-impact compression testing. Composites 1990;21(6):503–11.

[55] Caprino G, Lopresto V. On the penetration energy for fibre-reinforced plastics under low-velocity impact conditions. Compos Sci Technol 2001;61(1):65–73.

[56] Babic L, Dunn C, Hogg PJ. Damage development and its significance in GRP subjected to impact. Plast Rub Proc Appl 1989;12:199–207.

[57] Giurgiutiu V, Soutis C. Enhanced composites integrity through structural health monitoring. Appl Compos Mater 19(5):813–829.